Proc. Natl. Acad. Sci. USA
Vol. 82, pp. 1701–1705, March 1985
Biophysics

Opacification of γ-crystallin solutions from calf lens in relation to cold cataract formation

(eye/protein aging/phase diagram/quasielastic light scattering/coexistence curve)

ROLAND J. SIEZEN*, MICHAEL R. FISCH*, CHRISTINE SLINGSBY†, AND GEORGE B. BENEDEK*

*Department of Physics, Center for Materials Science and Engineering, Massachusetts Institute of Technology, Cambridge, MA 02139; and †Department of Crystallography, Birkbeck College, University of London, London WC1E 7HX, United Kingdom

Contributed by George B. Benedek, November 13, 1984

ABSTRACT **To determine the molecular mechanisms for cold cataract formation in the nucleus of the young mammalian lens, we have investigated the thermally reversible opacification of γ-crystallin solutions isolated from calf lens. Coexistence curves (plots of opacification temperature T_c versus protein concentration) were determined for the individual γ-crystallin fractions II, III, and IV as well as for the unfractionated γ-crystallin mixtures isolated from the nucleus and cortex. The coexistence curve of γIV-crystallin is remarkably elevated above those of γII- and γIII-crystallin and the γ-crystallin mixtures. The γIV-crystallin fraction is the major determinant of the opacification temperature within the whole lens or isolated cytoplasm. Quasielastic light-scattering spectroscopy of γIV-crystallin solutions indicates that above T_c there are two populations of protein aggregates of distinctly different mean size. As the temperature is lowered towards T_c, both populations increase in size. Opacification occurs when the population of large scatterers, which is composed of <0.1% protein by weight, reaches an average radius of about 20,000 Å.**

The cytoplasm in eye lens cells contains a highly concentrated solution of lens-specific proteins, the crystallins. Their concentration increases from ≈250 to 400 g/liter going from cortex to nucleus, thus establishing the refractive index gradient required for proper focusing of incident light (1). The cytoplasm is normally transparent because of short-range ordering of the crystallins (2, 3). Mammalian lenses contain primarily α-crystallins ($M_r \approx$ 700,000–1,200,000), β-crystallins ($M_r \approx$ 50,000–300,000) and γ-crystallins ($M_r \approx$ 20,000) (1, 4, 5). Their relative proportions vary with age and location within the lens as a result of both differential synthesis during development and selective degradation and insolubilization with aging (4–15). The lens nucleus is highly enriched in γ-crystallins, which are monomeric, basic proteins rich in sulfhydryl groups (8, 16–19). The majority of human cataracts represent an irreversible opacification of the lens nucleus that progresses with age, a condition that is accompanied by oxidation of sulfhydryl groups, aggregation, and insolubilization of the various crystallins (4, 8, 13, 20–23).

The cold cataract phenomenon observed in most young mammalian lenses (e.g., calf, rat, and rabbit) is a convenient model system to study the relationship between nuclear opacification and γ-crystallin aggregation. A temperature-dependent reversible opacification can be induced in the nucleus of these young lenses (24–28). This behavior appears to be an intrinsic property of the concentrated mixture of crystallins, since it also can be induced in purified, membrane-free cytoplasmic extracts of lens nucleus (27, 29–32). Cold cataract has been modeled as a reversible phase-separation phenomenon (26–32). Upon lowering the temperature below a critical value T_c, the cytoplasm separates into protein-rich and protein-poor domains. The spatial fluctuations in the index of refraction associated with these domains scatter incident light very effectively and thereby produce opacification. Domains with a radius of a few hundred nanometers have been identified both in opacifying calf lens and isolated nuclear cytoplasm by using quasielastic light scattering spectroscopy and electron microscopy (30, 33).

It has long been known that purified γ-crystallin solutions from rat and calf lens can cryoprecipitate reversibly (24, 25). Suggestions that cold cataract formation is related directly to γ-crystallin aggregation have been supported by findings that the cryoprecipitated phase is enriched in γ-crystallin (25, 33). Recent qualitative studies indicate that the individual γ-crystallin fractions II, III, and IV (and their subcomponents) differ in their cryoprecipitation behavior (19). This suggests that a more subtle relationship may exist between cold cataract formation and the relative concentration of individual γ-crystallin fractions. In the present study we have determined: (*i*) the coexistence curves of the native γ-crystallin mixtures isolated from either calf lens cortex or nucleus; (*ii*) the coexistence curves of each of the individual, purified γ-crystallin fractions γII, γIII, and γIV; (*iii*) the relative proportions of the various γ-crystallin fractions for the two coexisting phases along the phase boundaries obtained in *i*; and (*iv*) the size of the scattering elements responsible for opacification of γIV-crystallin solutions near its coexistence curve.

We present compelling evidence that the cold cataract phenomenon, which is seen only in the young lens nucleus and not in lens cortex or aged lens nucleus, is directly related to the concentration of γIV-crystallin.

MATERIALS AND METHODS

Protein Solutions. Lenses (0.9–1.0 g) from 1- to 2-week-old calves were separated into cortex (70–80% of lens volume) and nucleus (20–30%) and were extracted as before (34). The composition of the soluble lens proteins was determined by HPLC analysis (35) and is presented in Table 1.

The γ-crystallins were isolated by gel filtration on a Sephadex G-75 column (7). When required, the mixture of γ-crystallins was further separated into fractions I, II, III, and IV on sulfopropyl-(SP)-Sephadex C-50 (16). No further separation into subfractions IIIa and IIIb or IVa and IVb was attempted (12, 16, 17, 19). Purified fractions II, III, and IV were stored frozen at −20°C, in NaOAc buffer (pH 5.0) with 1 mM 2-mercaptoethanol, no distinction being made whether they were isolated from cortex or nucleus.

Just prior to phase-diagram measurements, each γ-crystallin fraction was thawed; dialyzed against 0.05 M phosphate buffer (pH 7.0; ionic strength, 0.11), thereby removing reducing agent; filtered through a 0.22-μm Millipore membrane; and reconcentrated as required in an Amicon B-15

The publication costs of this article were defrayed in part by page charge payment. This article must therefore be hereby marked "*advertisement*" in accordance with 18 U.S.C. §1734 solely to indicate this fact.

Abbreviation: QLS, quasielastic light scattering.

Table 1. Composition of soluble crystallins from calf lens cortex and nucleus

Soluble crystallins	Crystallin composition, %	
	Cortex	Nucleus
Total crystallin composition		
α-Crystallins	40	40
β-Crystallins	43	30
γ-Crystallins*	17	30
γ-Crystallin composition		
γI-Crystallin	7	6
γII-Crystallin	43	34
γIII-Crystallin	28	31
γIV-Crystallin	22	29

*HPLC analysis on TSK3000SW did not separate β_s-crystallin ($M_r \approx 22{,}000$) from γ-crystallins ($M_r \simeq 20{,}000$). Therefore, the amount of γ-crystallins is slightly overestimated, particularly in the cortex where β_s-crystallin is most abundant (7).

miniconcentrator. Samples were spun at 10,000 × *g* for 15 min at a temperature well above the opacification temperature, T_c, to remove any residual dust. After light scattering or transmission measurements, the protein concentrations were measured spectrophotometrically at 280 nm using an average $A^{1\%}_{1\,cm}$ value of 21 for all γ-crystallin fractions (17).

Determination of Opacification Temperature. A helium/neon laser (λ = 632.8 nm) was focused on the center of a small glass tube containing 100–150 μl of protein solution, and the intensity of transmitted light, I_t, was measured as a function of temperature with use of the equipment and procedures as described (29, 30). After we measured the maximal transmitted intensity, I_{max}, of the completely transparent protein solution at high temperature in the single-phase region, the temperature was lowered in increments of 0.2–2.0°C until the onset of opacification. The opacification temperature, T_c, was defined as the temperature for which I_t falls to 90% of the I_{max} (29, 30). For any sample studied, the T_c value could be repeatedly reproduced with an accuracy of ±0.5°C.

Separation of Protein-Rich and Protein-Poor Phases. A solution of nuclear γ-crystallins (42 g/liter) was cooled at 5°C for several days. The two phases were then separated by centrifugation (4400 × *g* for 10 min) in a Beckman J21B centrifuge at 5°C. Immediately after centrifugation, the clear supernatant was poured off, and the opaque protein-rich dense phase was redissolved in 0.05 M sodium phosphate buffer (pH 7.0). Subsequently, the composition of both phases was determined by SP-Sephadex ion-exchange chromatography.

Quasielastic Light Scattering. The temporal autocorrelation function $C(\tau)$ of the light scattered by γIV-crystallin solutions was measured for various protein concentrations as a function of decreasing temperature until T_c was reached. The equipment and procedures used have been described (29, 30). The resulting correlation functions could be fit quite well to the square of the sum of two exponentials (30), a form consistent with two distinct types of scatterers:

$$C(\tau) = (i_1 e^{-\tau/\tau_1} + i_2 e^{-\tau/\tau_2})^2 + B \qquad [1]$$

Here i_1 and i_2 are the intensities scattered by the first and second type of scatterers, τ_1 and τ_2 are the corresponding correlation times, and B is the baseline (30). The measured correlation times τ_1 and τ_2 differ by at least an order of magnitude. A cumulants fit of the data, based upon a polydisperse monomodal distribution of protein molecules, was not satisfactory.

The τ_1 and τ_2 values obtained from the correlation function can be related to the mean hydrodynamic radii $\bar{R}_h$ of the corresponding protein aggregates by the Stokes–Einstein relationship:

$$\frac{1}{\tau} = \bar{D}\, q^2 = \frac{k_B T\, q^2}{6\pi\eta \bar{R}_h} \qquad [2]$$

where k_B is Boltzman's constant, T is the absolute temperature, η is the solution viscosity (taken to be that of water), $\bar{D}$ is the mean diffusion coefficient, and $q = (4\pi n/\lambda)\sin(\theta/2)$ in which n is the index of refraction of the sample and λ is the light wavelength. In our experiments, $q = 2.5 \times 10^5\ cm^{-1}$. Eq. 2 provides a good measure of the size of the proteins or protein aggregates, provided that aggregate–aggregate interaction can be neglected.

The relative weight fractions of the protein molecules associated with the two populations can be deduced from the amplitudes i_1 and i_2 as follows. The fraction of light scattered by each population is $G_1 = i_1/(i_1 + i_2)$ and $G_2 = i_2/(i_1 + i_2)$. Experimentally we observed that $G_1 \simeq G_2 \simeq 0.5$. It can be shown (36) that the weight fraction $W_1 = M_1/(M_1 + M_2)$ is given by

$$W_1 = (G_1/M_1P_1)/[(G_1/M_1P_1) + (G_2/M_2P_2)] \qquad [3]$$

with corresponding expressions for W_2. We estimated P_2, the structure factor (30, 37), by assuming spherical aggregates of radius $(\bar{R}_h)_2$ using existing tables (37); P_1 is essentially unity. Our estimates for $P_2(90°)$ at various temperatures are in the range $0.001 < P_2(90°) < 0.8$ as $0°C < (T - T_c) < 20°C$.

RESULTS AND DISCUSSION

Coexistence Curves of γ-Crystallins from Cortex and Nucleus. Nuclear and cortical γ-crystallins from calf lens were isolated separately, and their opacification behavior was determined in 0.05 M sodium phosphate buffer (pH 7.0; ionic strength, 0.11). Fig. 1 shows characteristic plots of relative transmittance vs. temperature for various concentrations of nuclear γ-crystallins. From these we determined the opacification temperature T_c for each concentration. For freshly prepared samples, the transitions are fully reversible and very sharp, the transmitted intensity decreasing to <20% of I_{max} within 1°C. Similar sharp transitions are observed in isolated nuclear cytoplasm (27–30).

When the measured T_c values were plotted vs. protein concentration as in Fig. 2, we obtained the coexistence curve for nuclear γ-crystallins. In a similar way we determined the coexistence curve for the cortical γ-crystallin mix-

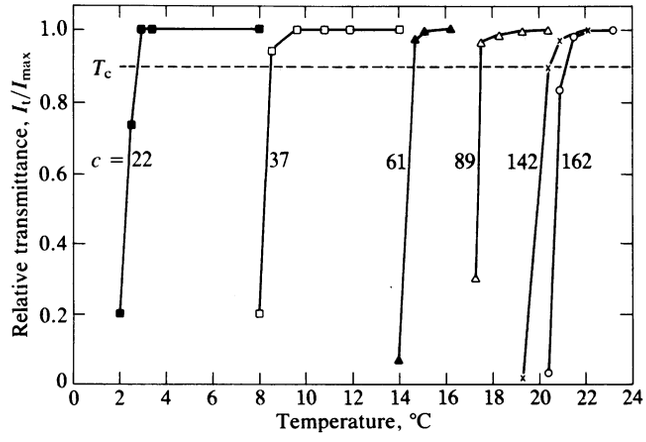

FIG. 1. Temperature dependence of the transparency of solutions of γ-crystallins from calf lens nucleus. Relative transmittance of solutions with concentration c in g/liter (as indicated) in 0.05 M phosphate buffer (pH 7.0) is plotted. The opacification temperature T_c is defined as the temperature at which the relative transmittance falls to 0.9.

ture. In this diagram the coexistence curve represents the boundary between the clear, single-phase region (above the curve) and the opaque region where the separated phases coexist. On both curves a maximum T_c value appears to be reached: at 14°C for cortical and 21°C for nuclear γ-crystallins. At the higher concentrations, the T_c values for cortical γ-crystallins decreased slightly. This is similar to the behavior of isolated nuclear cytoplasm (27, 29) and is characteristic of phase separations in a binary mixture (38, 39).

This data permits us to interpret the dramatic difference in the opacification temperature for nuclear cytoplasm as compared to cortical cytoplasm. The concentration of γ-crystallins increases progressively from the outer cortex to the inner nucleus of the calf lens. It can be shown that the γ-crystallin concentration is in the range of 30–60 g/liter in the cortex and 60–120 g/liter in the nucleus (1, 9–11, 27, 30, 31). The corresponding T_c values, read from Fig. 2, would be 2–7°C for cortical γ-crystallins and 15–20°C for nuclear γ-crystallins. This predicted difference in T_c values between γ-crystallins in cortex and nucleus agrees well with the observed difference in opacification behavior within the whole calf lens cortex ($T_c < 0$°C) and nucleus (13°C $< T_c <$ 19°C). This calculation demonstrates clearly that γ-crystallins play the central role in establishing the difference in phase separation between nucleus and cortex.

The coexistence curve for nuclear γ-crystallins is consistently 4–8°C higher than the curve for cortical γ-crystallins (Fig. 2). This difference in T_c must be related to the compositional difference between γ-crystallin mixtures isolated from cortex and nucleus, which we present in Table 1. The major differences are as follows. The fraction of γIV-crystallin increases from 22% in the cortex to 29% in the nucleus, whereas γII decreases from 43% to 34%. It was recently shown by one of us (C.S.) that γIVa-, γIVb-, and γIIIa-crystallin cryoprecipitated at 0°C, while γII- and γIIIb-crystallin did not (19). Thus, we have reason to believe that the T_c for γ-crystallin solutions will rise with an increase in the relative proportion of γIV-crystallin (and possibly γIIIa-crystallin). To investigate this effect in greater detail, we determined the coexistence curves for the three main components γII-, γIII-, and γIV-crystallin.

Coexistence Curves of Individual γ-Crystallins. The coexistence curves of the individual purified γ-crystallins, as measured in 0.05 M phosphate buffer (pH 7.0), are given in Fig. 3. These curves were all reproducible with different batches of γ-crystallins, and all transitions were fully reversible upon temperature cycling. The minor, heterogeneous γI-crystallin fraction (16) was not considered.

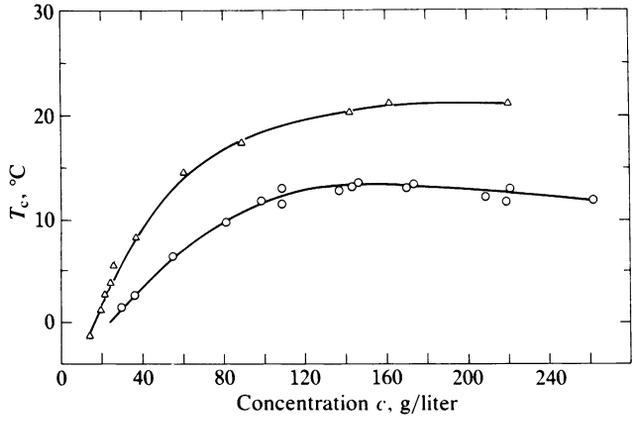

FIG. 2. Coexistence curves for phase separation of γ-crystallins from calf lens cortex (○) and nucleus (△) in 0.05 M phosphate buffer (pH 7.0). Above each curve the solutions are transparent ($I_t/I_{max} >$ 0.9), whereas below each curve the solutions are opaque ($I_t/I_{max} <$ 0.9) due to phase separation.

Fig. 3 shows that the coexistence curves for each of these pure γ-crystallin fractions are dramatically different. It is important to observe that the data of γII-crystallin shows a characteristic double-valued, bell-shaped curve. This is the hallmark of binary phase separation (38, 39). Based on this observation, we would expect that the curve for γIII-crystallin will turn downward at sufficiently high concentration. It is remarkable that the curve for γIV-crystallin is so much higher than those of γII and γIII. Indeed, the data indicates that the maximum phase-separation temperature for pure γIV-crystallin is well in excess of body temperature.

We may use the data shown in Fig. 3 to estimate the net effect of each of the individual γ-crystallin fractions on the phase separation of mixtures. Table 2 lists our estimates of the average concentration of each γ-crystallin in calf lens cortex and nucleus and the corresponding T_c values obtained from Fig. 3. Using this data, we can attempt to explain the opacification temperatures observed in whole lens, isolated cytoplasm, and the unfractionated γ-crystallin mixtures. The concentration and corresponding T_c values of γII- and γIII-crystallin (Table 2, rows 2 and 3) are clearly too low to account for the opacification temperatures of the γ-crystallin mixtures from cortex and nucleus (Table 2, row 5). On the other hand, the T_c values associated with the average concentrations of γIV-crystallin are very close to the T_c values measured for native γ-crystallin mixtures. This strongly suggests that T_c for these mixtures is largely determined by the absolute concentration of γIV-crystallin.

It is remarkable that in whole lens and isolated cytoplasm, the observed T_c values, both cortical and nuclear, are only slightly lower than those produced by the γ-crystallin mixture alone. Keeping in mind the fact that the γ-crystallins constitute <30% of the total protein in the cytoplasm of whole lens, they nevertheless appear to largely define the conditions for phase separation.

Composition of Protein-Rich and Protein-Poor Phases of γ-Crystallins. To understand the nature of this phase separation phenomenon, it is clearly desirable to determine the composition of the constituent proteins in the separated phases.

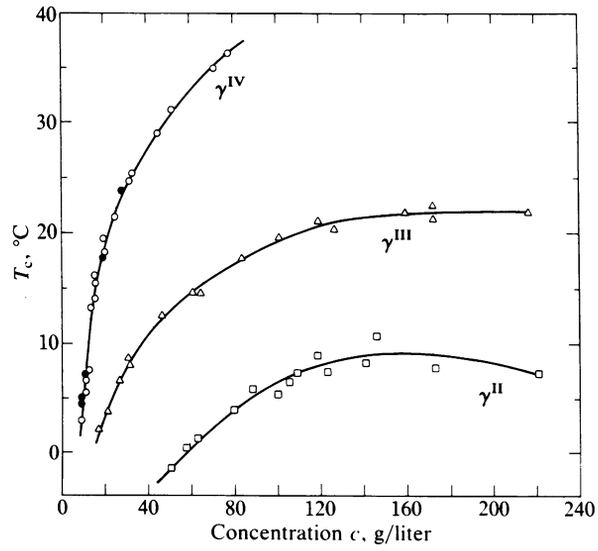

FIG. 3. Coexistence curves for isolated γII- (□), γIII- (△), and γIV-crystallin (○, ●) at pH 7.0 (ionic strength, 0.11). Open symbols designate phosphate buffer; closed symbols designate Tris buffer. These coexistence curves can be shifted upward or downward by variations of pH or ionic strength and by the addition of various chemical reagents (40). For example, 1 mM reducing agent (dithiothreitol or glutathione) shifts the coexistence curve of γIV down by about 2°C.

Table 2. Calf lens γ-crystallins: Estimated physiological average concentration and opacification temperature in cortex and nucleus

Crystallins	Cortex crystallins		Nucleus crystallins	
	Concentration,* g/liter	T_c,† °C	Concentration,* g/liter	T_c,† °C
	Individual γ-crystallins			
γI-Crystallin	3		6	
γII-Crystallin	19	<0	30	<0
γIII-Crystallin	13	0	28	7
γIV-Crystallin	10	5	26	22
	Crystallin mixtures			
Unfractionated γ-crystallins	45	4	90	18
Isolated cytoplasm‡		<0		10–15
Whole lens‡		<0		13–19

*The average concentrations were estimated from observed γ-crystallin compositions as a function of lens age and radius (refs. 1, 9–11, and 27; also our own unpublished data).
†The corresponding T_c values for γ-crystallin solutions were obtained from the coexistence curves in Figs. 2 and 3.
‡Literature values for T_c in whole lens (26, 30) and undiluted cytoplasm (29–32) are also given.

We cooled a mixture of nuclear γ-crystallins (42 g/liter) to 5°C and subsequently separated the clear (protein-poor) and opaque (protein-rich) phases by centrifugation. Analysis of the γ-crystallin composition of these phases, as presented in Table 3, shows that both the opaque and clear phases contain all four γ-crystallin fractions.

However, the compositions of the two phases are distinctly different, the opaque phase being highly enriched in γIV-crystallin and depleted of γII-crystallin (γIV/γII = 2.1) relative to the original mixture (γIV/γII = 0.85). Analogous results were obtained upon separation of opacified γ-crystallin solutions from calf lens cortex.

Size of the Scattering Units in γIV-Crystallin Solutions. We measured the temporal autocorrelation function of the light scattered from pure γIV-crystallin solutions as a function of temperature at different protein concentrations. At each temperature we found that the scattering was produced by two distinct populations of protein aggregates. In Fig. 4 we plot the mean hydrodynamic radii $\overline{R}_h$ of both populations vs. $T - T_c$ for each of the protein concentrations studied. It is important to note that the value of T_c changes for each protein concentration according to the coexistence curve in Fig. 3. Nevertheless, it is remarkable that the hydrodynamic radius of each population is approximately the same function of $T - T_c$ for each of the protein concentrations studied (Fig. 4). The population distributions and mean sizes were found to be essentially reversible upon temperature cycling.

We observe from Fig. 4 that, as the temperature is lowered towards the coexistence curve, the size of the small scatterers increases from 30 to 90 Å mean radius as $T - T_c$ goes from 20°C to 0°C. These small scatterers presumably correspond to γIV-crystallin monomers (R_h = 20 Å; ref. 41) in reversible equilibrium with small oligomers. Such a reversible self-association of total γ-crystallins has been detected by frontal gelchromatography by Siezen and Owen (41). The population of large scatterers is polydisperse and the mean

Table 3. Composition of protein-rich and protein-poor phases of phase-separated nuclear γ-crystallins

Individual γ-crystallin	Initial mixture, %	Dilute phase at 5°C, %	Dense phase at 5°C, %
γI-Crystallin	6	7	4
γII-Crystallin	34	40	21
γIII-Crystallin	31	31	30
γIV-Crystallin	29	22	45

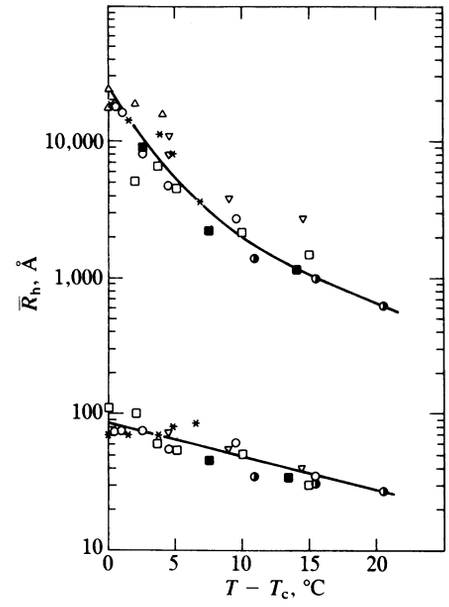

FIG. 4. Mean hydrodynamic radii ($\overline{R}_h$) of the small and large scattering units in γIV-crystallin solutions as a function of temperature (T_c to T_c + 20°C). The radii were calculated from the respective correlation times τ_1 and τ_2 with Eq. 2. The ordinate is a logarithmic scale. Protein concentrations are 9.9 (■), 15.1 (□), 16.0 (◑), 23.8 (▽), 29.5 (○), 49.2 (*), and 71.5 g/liter (△).

size increases dramatically from ≈600 to 20,000 Å as $T - T_c$ changes from 20°C to 0°C. These large scatterers are clearly responsible for the opacification of the solution, since their mean size is comparable to the wavelength of the incident light.

The weight fraction of the small scatterers, W_1, was estimated by using Eq. 3 and the radii from Fig. 4. This admittedly crude calculation indicates that 99.9% or more by weight of the γIV-crystallin remains in the population of small scatterers over the entire temperature range as T_c is approached. Thus, a relatively small number of very large γ-crystallin particles or aggregates, almost negligible by weight, dominates the scattering behavior of the entire γ-crystallin solution, ultimately leading to complete opacification.

The existence of two distinct populations in the time correlation functions, at temperatures above T_c, is quite different from that expected from a simple binary phase transition. Further experiments are needed to clarify the precise nature of the phase separation occurring in this complex system.

GENERAL DISCUSSION

A major point that emerges from this work is that the opacification temperature of calf lens γ-crystallin solutions is largely determined by the concentration of γIV-crystallin present. Its coexistence curve lies well above those of the other γ-crystallins, and this curve is particularly steep in the physiological range of γIV-crystallin (up to 40 g/liter). This steepness suggests that small variations in γIV-crystallin concentration within the lens should have a large effect on the opacification temperature T_c.

In the young bovine lens, it is only the nucleus that exhibits "cold cataract." There is ample evidence that γIV-crystallin is most concentrated in the nucleus (refs. 6–8 and 12; also this work) as a result of the high synthesis of γIV-crystallin during embryonic development (6, 7). Mature bovine lenses do not exhibit nuclear cold cataract, even though the soluble protein fraction is highly enriched in γ-crystallins. Blundell *et al.* (19) even observed that the soluble proteins of the innermost region of the adult bovine lens consist nearly

entirely of γ-crystallins. With aging, selective aggregation and insolubilization removes α- and β-crystallins from the soluble fraction (9–11). Our data suggests that the absence of cold cataract in the adult nucleus may result from the fact that the aged nucleus contains very little γIV-crystallin and reduced levels of γIII-crystallin (7, 12). This selective depletion of γIV-crystallin (and γIII) could result from either degradation with aging or, more likely, insolubilization due to interaction with the aggregating high molecular weight α- and β-crystallins or with plasma membranes (23).

Human senile nuclear cataract formation is accompanied by insolubilization of low molecular weight crystallins (4, 13, 22). Clearly it would be desirable to measure the absolute concentrations and coexistence curves of each of the γ-crystallin species in normal and cataractous human lenses of different age. In this connection it is interesting to note that in galactose-induced cataract in rats, the opacification is accompanied by a marked change in the relative proportions of soluble γ-crystallin fractions (42).

Additional support for the central role played by γIV-crystallin in nuclear opacification is provided by our analyses of the size distribution of γIV-crystallin scattering units as T_c is approached. Two distinctly different size populations of scatterers were found in γIV-crystallin solutions. This behavior is markedly similar to that occurring at the onset of opacification in both whole lens and isolated nuclear cytoplasm (30). In each case, the large scattering elements determine the opacification behavior of the system.

An intriguing question arises as to the nature of the structural differences between γII-, γIII- and γIV-crystallins (and their subfractions) that lead to such large variations in opacification behavior. Their amino acid compositions are very similar, and their primary sequences are highly homologous (8, 16, 17, 43, 44). Three-dimensional structure analysis by x-ray diffraction of γII-, γIIIa-, γIIIb-, and γIV-crystallin has either been reported or is in progress (19, 45–47). There is sufficient evidence that all have the same highly symmetrical, two-domain, antiparallel β-sheet backbone structure as described in detail for γII-crystallin (45–47). The surface characteristics of individual γ-crystallins will then contribute to the differences in their cryoprecipitation behavior. γII-Crystallin has a highly-ordered surface distribution of negative and positive charges, mainly aspartates and arginines (46, 47). It will be essential to determine whether this distribution is retained or modified in the other γ-crystallin fractions.

There are some known differences in the surface structure. The number of exposed -SH groups (and the total -SH content) appears to decrease in the order γII > γIII > γIV (16). In addition, near-ultraviolet circular dichroism measurements show that γII-, γIII-, and γIV-crystallin have subtle differences in the environment of their aromatic residues and/or disulfide bridges (48). Such differences in the exposure of aromatic and sulfhydryl groups may well account for the variations in T_c observed for the various γ-crystallin fractions.

We thank Beth Kaplan for her excellent technical assistance and Jack Leifer, Bob Anello, and Chris Coppin for their enthusiastic participation in this project as part of the Massachusetts Institute of Technology Undergraduate Research Opportunities Program. This research was supported by the National Eye Institute of the National Institutes of Health under Grant RO1-EY05127.

1. De Jong, W. W. (1981) in *Molecular and Cellular Biology of the Eye Lens*, ed. Bloemendal, H. (Wiley, New York), pp. 221–278.
2. Benedek, G. B. (1971) *Appl. Opt.* **10,** 459–473.
3. Delaye, M. & Tardieu, A. (1983) *Nature (London)* **302,** 415–417.
4. Harding, J. J. & Dilley, K. J. (1976) *Exp. Eye Res.* **22,** 1–73.
5. Bindels, J. G., Bessems, G. J., De Man, B. M. & Hoenders, H. J. (1983) *Comp. Biochem. Physiol. B* **76,** 47–55.
6. Papaconstantinou, J. (1965) *Biochim. Biophys. Acta* **107,** 81–90.
7. Slingsby, C. & Croft, L. R. (1973) *Exp. Eye Res.* **17,** 369–376.
8. Croft, L. R. (1973) in *The Human Lens in Relation to Cataract*, CIBA Foundation Symposium 19, eds. Elliott, K. & Fitzsimons, D. W. (Elsevier, Amsterdam), pp. 207–226.
9. Van Kamp, G. J. & Hoenders, H. J. (1973) *Exp. Eye Res.* **17,** 417–426.
10. Bours, J. (1980) *Anal. Chem. Symp. Ser.* **5,** 207–220.
11. Hoenders, H. J. & Bloemendal, H. (1981) in *Molecular and Cellular Biology of the Eye Lens*, ed. Bloemendal, H. (Wiley, New York), pp. 279–326.
12. Slingsby, C. & Miller, L. R. (1983) *Exp. Eye Res.* **37,** 517–530.
13. Bessems, G. J., Hoenders, H. J. & Wollensak, J. (1983) *Exp. Eye Res.* **37,** 627–637.
14. Bindels, J. G., Bours, J. & Hoenders, H. J. (1983) *Mech. Ageing Dev.* **21,** 1–13.
15. Bours, J. (1984) *Curr. Eye Res.* **3,** 691–697.
16. Björk, I. (1964) *Exp. Eye Res.* **3,** 254–261.
17. Björk, I. (1970) *Exp. Eye Res.* **9,** 152–157.
18. Bours, J., Vornhagen, R., Herlt, M. & Rink, H. (1982) *Curr. Eye Res.* **1,** 651–658.
19. Blundell, T. L., Lindley, P. F., Miller, L. R., Moss, D. S., Slingsby, C., Turnell, W. G. & Wistow, G. (1983) *Lens Res.* **1,** 109–131.
20. Anderson, E. I. & Spector, A. (1978) *Exp. Eye Res.* **26,** 407–417.
21. Augusteyn, R. C. (1981) in *Mechanisms of Cataract Formation in the Human Lens*, ed. Duncan, G. (Academic, New York), pp. 71–115.
22. Harding, J. J. (1981) in *Molecular and Cellular Biology of the Eye Lens*, ed. Bloemendal, H. (Wiley, New York), pp. 327–365.
23. Garner, W. H., Garner, M. H. & Spector, A. (1981) *Biochem. Biophys. Res. Commun.* **98,** 439–447.
24. Zigman, S. & Lerman, S. (1965) *Exp. Eye Res.* **4,** 24–30.
25. Lerman, S., Zigman, S. & Forbes, W. F. (1966) *Biochem. Biophys. Res. Commun.* **22,** 57–61.
26. Benedek, G. B., Clark, J. I., Serrallach, E. N., Young, C. Y., Mengel, L., Sauke, T., Bagg, A. & Benedek, K. (1979) *Philos. Trans. R. Soc. London Ser. A* **293,** 329–340.
27. Clark, J. I. & Benedek, G. B. (1980) *Biochem. Biophys. Res. Commun.* **95,** 482–489.
28. Clark, J. I., Neuringer, J. R. & Benedek, G. B. (1983) *J. Geront.* **38,** 287–292.
29. Delaye, M., Clark, J. I. & Benedek, G. B. (1981) *Biochem. Biophys. Res. Commun.* **100,** 908–914.
30. Delaye, M., Clark, J. I. & Benedek, G. B. (1982) *Biophys. J.* **37,** 647–656.
31. Clark, J. I., Delaye, M., Hammer, P. & Mengel, L. (1982) *Curr. Eye Res.* **1,** 695–704.
32. Hammer, P. & Benedek, G. B. (1983) *Curr. Eye Res.* **2,** 809–814.
33. Gulik-Krzywicki, T., Tardieu, A. & Delaye, M. (1984) *Biochim. Biophys. Acta* **800,** 28–32.
34. Siezen, R. J., Bindels, J. G. & Hoenders, H. J. (1979) *Exp. Eye Res.* **28,** 551–567.
35. Horwitz, J., Ding, L. L. & Cheung, G. C. (1983) *Lens Res.* **1,** 159–174.
36. Mazer, N. A., Benedek, G. B. & Carey, M. C. (1976) *J. Phys. Chem.* **80,** 1075–1085.
37. Denman, H. H., Heller, W. & Pangonis, W. J. (1966) *Angular Scattering Functions for Spheres* (Wayne State Univ. Press, Detroit, MI), pp. 127–168.
38. Flory, P. J. (1953) *Principles of Polymer Chemistry* (Cornell Univ. Press, Ithaca, NY), pp. 541–548.
39. Stanley, H. E. (1971) *Introduction to Phase Transitions and Critical Phenomena* (Clarendon, Oxford).
40. Siezen, R. J., Fisch, M. R. & Benedek, G. B. (1984) *Proceedings of the International Society for Eye Research*, ed. Belmonte, C. (Inter. Soc. Eye Res., New York), Vol. 3, p. 151 (abstr.).
41. Siezen, R. J. & Owen, E. A. (1983) *Biophys. Chem.* **18,** 181–194.
42. Wagner, B. J. & Fu, S.-C. J. (1978) *Exp. Eye Res.* **26,** 255–265.
43. Slingsby, C. & Croft, L. R. (1978) *Exp. Eye Res.* **26,** 291–304.
44. Moormann, R. J. M., Den Dunnen, J. T., Bloemendal, H. & Schoenmakers, J. G. G. (1982) *Proc. Natl. Acad. Sci. USA* **79,** 6876–6880.
45. Chirgadze, Y. N., Sergeev, Y. V., Fomankova, N. P. & Oreshin, V. D. (1981) *FEBS Lett.* **131,** 81–84.
46. Blundell, T., Lindley, P., Miller, L., Moss, D., Slingsby, C., Tickle, I., Turnell, B. & Wistow, G. (1981) *Nature (London)* **289,** 771–777.
47. Wistow, G., Turnell, B., Summer, L., Slingsby, C., Moss, D., Miller, L., Lindley, P. & Blundell, T. (1983) *J. Mol. Biol.* **170,** 175–202.
48. Horwitz, J., Kabasawa, I. & Kinoshita, J. H. (1977) *Exp. Eye Res.* **25,** 199–208.